NONLINEAR INTERACTIONS IN PRACTICAL WIND WAVE MODELS [1]

Hendrik L. Tolman[2] and
Vladimir M. Krasnopolsky[3]

SAIC/GSO at NOAA/NCEP/EMC
Marine Modeling and Analysis Branch
Camp Springs, Maryland, USA

1 INTRODUCTION

Ocean wave modeling has been in the center of interest for several decades. Following Hasselmann (1960) numerical models are generally based on an action or energy balance equation of the form

$$\frac{DF}{Dt} = S_{tot} = S_{in} + S_{nl} + S_{ds} \quad , \tag{1}$$

where F is the spectrum and S_{tot} represents the sources and sinks, consisting of a wind input (S_{in}), nonlinear interactions (S_{nl}) and dissipation (S_{ds}) source terms. Arguably the biggest breakthrough in the understanding of wind wave generation, and hence in numerical wave modeling, occurred with the understanding of the critical role of the nonlinear interactions source term S_{nl} in the process of wave growth (Phillips, 1960; Hasselmann, 1962, 1963a,b; Hasselmann et al., 1973). The nonlinear interactions are believed to provide the lowest order mechanism to shift wave energy to longer waves, and also provide a stabilization mechanism for the shape of the spectrum. Reviews of the interactions and their impact can be found, for instance, in Masuda (1980), Phillips (1981), Young and Van Vledder (1993) or Komen et al. (1994).

The exact computation of the nonlinear interactions S_{nl} involves the evaluation of a six-dimensional Boltzmann integral, which includes an interaction function with strong moving singularities (e.g., Webb, 1978; Herterich and Hasselmann, 1980). The dimensionality of the integral is effectively reduced due the fact that contributions exist only for so-called quadruplets of four spectral components with wavenumber vectors $\boldsymbol{k}_1$ through $\boldsymbol{k}_4$ and (radian) frequencies σ_1 through σ_4 ($\sigma = 2\pi f$) that satisfy the following resonance conditions (Hasselmann, 1962, 1963a) :

$$\boldsymbol{k}_1 + \boldsymbol{k}_2 = \boldsymbol{k}_3 + \boldsymbol{k}_4 \quad , \tag{2}$$

$$\sigma_1 + \sigma_2 = \sigma_3 + \sigma_4 \quad . \tag{3}$$

This effectively reduces the integral to a three-dimensional integral. However, even with present day computer technology, and with various improvements in the efficiency of the computation of these integrals (e.g., Masuda, 1980; Tracy and Resio, 1982; Resio and Perrie, 1991; Komatsu and Masuda, 1996; Van Vledder, 2000) the exact integral is prohibitively expensive for use in practical models.

From the perspective of practical wave modeling, a major breakthrough occurred with the development of the Discrete Interaction Approximation (DIA, Hasselmann et al., 1985), which proved sufficiently economical for application in operational wave models. The DIA achieves a massive speed up compared to the exact interaction in two ways. First only a single 'representative' quadruplet satisfying Eqs. (2), (3) is considered. This quadruplet is defined by

$$\left.\begin{array}{rcl} \boldsymbol{k}_2 & = & \boldsymbol{k}_1 \\ \sigma_3 & = & (1+\lambda)\sigma_1 \end{array}\right\} \quad , \tag{4}$$

where λ is a constant and $\boldsymbol{k}_1$ corresponds to discrete spectral components in the wave model only. For each $\boldsymbol{k}_1$ only two ('mirror image') quadruplets satisfy Eqs. (2), (3) and (4). Second, the exact interaction integral is replaced by a "deep water discrete-interaction analogue", which after some manipula-

[1] MMAB contribution Nr. 241
[2] E-mail:Hendrik.Tolman@NOAA.gov
[3] E-mail:Vladimir.Krasnopolsky@NOAA.gov

tion (see Hasselmann et al., 1985, for details) becomes (considering deep water for simplicity)

$$\begin{pmatrix} \delta S_{nl,1} \\ \delta S_{nl,3} \\ \delta S_{nl,4} \end{pmatrix} = \begin{pmatrix} -2 \\ 1 \\ 1 \end{pmatrix} C g^{-4} f_1^{11} \times \left[F_1^2 \left(\frac{F_3}{(1+\lambda)^4} + \frac{F_4}{(1-\lambda)^4} \right) - \frac{2 F_1 F_3 F_4}{(1-\lambda^2)^4} \right] , \quad (5)$$

where δS_{nl} represent the discrete contributions to S_{nl} for a given discrete spectral component $\boldsymbol{k}_1$, and where the suffices denote the spectrum and source term contributions at the four components of the quadruplet considered.

The DIA made the development of the first third-generation wave model possible (WAM, WAMDIG, 1988), where Eq. (1) is parameterized without assuming the resulting spectral shape. Nevertheless, even with the success of the DIA, Hasselmann et al. (1985) recognized shortcomings in the accuracy of the DIA. It is therefore not surprising that alternative parameterizations of S_{nl} have been the subject of much research in the past two decades.

In essence, three different approaches have been used to produce more accurate yet economical parameterizations of S_{nl}.

a) Simplification and/or speeding up of the exact interaction equations.
b) Improving the DIA.
c) Development of new technique's.

NOAA's National Centers for Environmental Prediction (NCEP) have been involved in the latter two lines of research, as will be described in more detail in the following sections. The present introduction will briefly discuss the efforts at other institutes.

The above approaches to speed up the exact interactions mostly consider using filtering techniques to reduce the number of computations, and hence speed the computations (e.g., Snyder et al., 1998; Hashimoto and Kawaguchi, 2001). In this context, Hashimoto and Kawaguchi (2001) present the SRIAM method, which is claimed to 'retain most of the [interaction's] accuracy in computing the nonlinear energy transfer' at about 20 times the costs of the DIA. Although this claim is not substantiated with actual model integrations, this approach appears to be promising.

Approaches based on making the DIA more accurate are closely related to the above methods to make the exact interactions more economical, as both intend to trade accuracy for economy or vise versa. Expansions to the DIA (e.g., Ueno and Ishizaka, 1997; Hashimoto and Kawaguchi, 2001; Van Vledder, 2001, 2002a), are discussed in Section 2.a. Several of the above papers indicate that much progress can be made while increasing the computational costs compared to the DIA by an order of magnitude or less. A recent review can be found in Tolman (2003, 2004), which will be used as the basis of the present study in Section 2. In this context it is also interesting to consider the studies by Polnikov and Farina (2002) and Polnikov (2003), who also address the economy of the DIA.

Other approaches have been suggested to economically parameterize S_{nl}. Many early approaches were fully parametric. Several of these are reviewed by Hasselmann et al. (1985). Generally, fully parametric methods are shown to either lack accuracy or the capability of stabilizing the shape of the spectrum. One of the methods presented by Hasselmann et al. (1985) is that of representing S_{nl} by a diffusion operator. Such an approach has more recently been pursued by Zakharov and Pushkarev (1999) and Jenkins and Phillips (2001). Whereas Zakharov and Pushkarev (1999) have shown the feasibility of such an approach in a third generation wave model, its accuracy and potential has not yet been extensively tested, and will not be addressed here.

A relatively new method to parameterize the nonlinear interactions is the use of Neural Networks (NN) as explored by Krasnopolsky et al. (2002) and Tolman et al. (2005). Although some progress has been made in this approach, this method has not yet matured sufficiently to be feasible in a practical wave model. Recent developments in this approach at NCEP will be discussed in Section 3. After this, a brief outlook will be presented in Section 4.

2 DIA APPROACHES

2.a Introduction

A recent review of most suggested modifications to the DIA is presented in Tolman (2003, 2004). Such modifications include:

a) Expand the DIA by adding more representative quadruplets. When $S_{nl,i}$ represents the

nonlinear interactions for one of these representative quadruplets, and when N quadruplets are selected, this multiple DIA or MDIA is defined as

$$S_{nl} = \frac{1}{N} \sum_{i=1,N}^{N} S_{nl,i} \quad . \tag{6}$$

b) Replace the definition of the quadruplet layout given by Eq. (4) to become more versatile. This will be discussed in more detail in Section 2.b.

c) Add more tunable proportionality constants to Eq. (5).

The appropriate references for all these previously suggested modifications to the DIA can be found in Tolman (2003, 2004). The latter papers furthermore introduce a so-called variable DIA (VDIA), where the parameters defining the DIA (traditionally λ and C) are allowed to vary in spectral space.

It should be noted that in this context, the methods of Polnikov and Farina (2002) and Polnikov (2003) to further speed up the DIA have not been considered, because these methods are directly linked to the discrete spectral resolution of a model. This is considered to be an undesirable feature for general purpose models by the present authors.

Tolman (2003, 2004) investigated the impact of these modifications to the original DIA using methodologies taken from previous studies. For a small number of parametrically defined spectra, the exact nonlinear interactions are calculated using the Web-Resio-Tracy (WRT) method (Webb, 1978; Tracy and Resio, 1982; Resio and Perrie, 1991), as implemented in software package developed by Van Vledder (2002b). The optimum parameter settings for each DIA are then obtained by minimizing the rms differences between the exact (WRT) and approximate (DIA) computations. From this study, the following conclusions were drawn:

1) To increase the accuracy of the DIA, it is of paramount importance to expand the definition of the representative quadruplet.

2) An MDIA with expanded quadruplet definition and $N = 4$ representative quadruplets can dramatically improve the performance of the DIA for selected spectra.

3) Adding additional proportionality constants to Eq. (5) does not appear useful. Small increases in accuracy are offset by increased noise in the solution.

4) The VDIA has only a minor positive impact compared to a similar DIA with constant components. It remains to be seen if the added complexity of the VDIA can be justified in light of its performance.

The above findings suggest that an MDIA with an expanded definition of the quadruplet has potential for improving the parameterization of the nonlinear interactions in practical wind wave models. However, the above studies also led to two alarming observations, that have guided much of the recent research at NCEP. First, it was found that not all alternative versions of the DIA result in stable model integration when applied in a practical wind wave model. Second, in spite of the massive improvements of individual interactions for individual spectra for an MDIA when compared to the original DIA, differences in model results when applied in a wave model appeared minimal.

The next sections will highlight results that have been obtained at NCEP since the publication of Tolman (2004). Conciseness forces us to focus mainly on the results. A full account of these experiments will be presented elsewhere.

2.b Defining a general MDIA

Ongoing research at NCEP has focused on several aspects of the DIA. First, a general deep water MDIA with the maximum flexibility of the quadruplet layout is defined to form the basis of further research. In principle, such an (M)DIA has already been defined by Van Vledder (2001). However, his quadruplet layout is not optimal from a numerical efficiency perspective for the following reasons.

When a quadruplet layout is defined, two issues are important. The first is the layout of the quadruplet as defined by, for instance, Eq. (4) in combination with the general resonance conditions (2) and (3). The second is the way in which this quadruplet layout is used to sample spectral space. Typically, the representative quadruplet is applied to each discrete wavenumber $\boldsymbol{k}_d$ making up the discrete spectral space. In the original DIA, the quadruplet is used to sample spectral space by choosing $\boldsymbol{k}_d = \boldsymbol{k}_1$. It can be shown that, in principle, the same interactions should be found if the spectral space is sampled by choosing $\boldsymbol{k}_d$ equal to any other component $\boldsymbol{k}_i$ of the quadruplet, or to arbitrary wavenumber vectors made up of a fixed linear combination of $\boldsymbol{k}_i$.

Differences between such approaches only occur due to different interpolation in discrete spectral space. Numerical experiments confirm that the choice of $\boldsymbol{k}_d$ within the above constraints has only a small impact on individual interactions, or on model integration.

The method of sampling for a given quadruplet layout impacts the numerical efficiency of the MDIA. Because a significant part of the computational effort of any DIA is used for interpolating in spectral space (e.g., Polnikov, 2003), it is prudent to choose the sampling method to minimize such interpolations. With this in mind, the following representative quadruplet and sampling method have been defined

$$\left.\begin{array}{rcl} \boldsymbol{k}_d & = & \frac{||\boldsymbol{k}_1||}{||\boldsymbol{k}_1+\boldsymbol{k}_2||}\,(\boldsymbol{k}_1+\boldsymbol{k}_2) \\ \sigma_1 & = & a_1\sigma_d \;=\; (1+\mu)\sigma_d \\ \sigma_2 & = & a_2\sigma_d \;=\; (1-\mu)\sigma_d \\ \sigma_3 & = & a_3\sigma_d \;=\; (1+\lambda)\sigma_d \\ \sigma_4 & = & a_4\sigma_d \;=\; (1-\lambda)\sigma_d \\ \theta_2 & = & \theta_1 \pm \Delta\theta \end{array}\right\} \quad , \qquad (7)$$

where $\sigma_d = 2\pi f_d$ is the frequency corresponding to $\boldsymbol{k}_d$. The contributions to the DIA corresponding to Eq. (5) become

$$\begin{pmatrix} \delta S_{nl,1} \\ \delta S_{nl,2} \\ \delta S_{nl,3} \\ \delta S_{nl,4} \end{pmatrix} = \frac{1}{2} \begin{pmatrix} -1 \\ -1 \\ 1 \\ 1 \end{pmatrix} C\, g^{-4} f_d^{11} \times \left[\frac{F_1 F_2}{(a_1 a_2)^4} \left(\frac{F_3}{a_3^4} + \frac{F_4}{a_4^4} \right) - \frac{F_3 F_4}{(a_3 a_4)^4} \left(\frac{F_1}{a_1^4} + \frac{F_2}{a_2^4} \right) \right] , \qquad (8)$$

The quadruplet is defined by three parameters λ, μ and $\Delta\theta$ and generally four layouts are found for each setting of these parameters. To assure that this DIA reduces to the traditional DIA with 2 solutions for the representative quadruplet, the factor $\frac{1}{2}$ is added. The corresponding MDIA remains defined as in Eq. (6).

It can be shown that the quadruplet layout (7) is identical to the layout of Van Vledder (2001), except for the way in which spectral space is sampled. However, the number of discrete spectral points involved in evaluating contributions to S_{nl} for a given $\boldsymbol{k}_d$ is reduced from 41 in the approach of Van Vledder (2001), to 28 in Eqs. (7). In principle, this redefinition is expected to speed up the corresponding part of the computations by approximately 30% due to a corresponding reduction in the necessary mathematical operations.

Note that the MDIA defined by Eqs. (6) through (8) reduces to the traditional DIA for $N = 1$, $\mu = 0$ and $\Delta\theta = 0°$ [considering that even then there are in principle 4 solutions to Eq. (7), whereas there are only two solutions to Eq. (4)]. This quadruplet definition reduces to the two parameter (λ, μ) quadruplet of Tolman (2004) by choosing $\boldsymbol{k}_d = \frac{1}{2}(\boldsymbol{k}_1 + \boldsymbol{k}_2)$ and $\sigma_d = \frac{1}{2}(\sigma_1 + \sigma_2)$, in which case $\Delta\theta$ is implicitly defined. In the following, these definitions will be used to describe the one-parameter (λ), two-parameter (λ, μ) and three-parameter $(\lambda, \mu, \Delta\theta)$ quadruplets, respectively.

2.c Stability of integration

The second subject of further investigation at NCEP has been the issue of the stability of the model integration for several MDIAs. By testing the DIA for selected spectra only, many previous authors appear to have assumed implicitly that any DIA would result in successful model integration. The results presented in (Tolman, 2003) show that such an assumption would be erroneous. In the latter study, alternative MDIAs were incorporated in the wave model WAVEWATCH III (Tolman, 2002; Tolman et al., 2002), while otherwise using the default set-up of this model. By running time limited wave growth tests, where Eq. (1) is reduced to

$$\frac{\partial F}{\partial t} = S_{tot} \quad , \qquad (9)$$

it was shown that an optimized MDIA with a single two-parameter representative quadruplet results in unstable model integrations.

Since the publication of the above report and its companion paper, these time limited growth tests have been expanded to investigate the model integration stability for a wider range of alternative MDIAs. For MDIAs with a single representative quadruplet, it was shown that only the traditional quadruplet layout results in stable model integration for a broad range of parameter settings. For all multi-parameters definitions of the quadruplet, the model integration was found to be systematically unstable for significant parts of the parameter space for which valid quadruplets exist.

Convincing explanations for this behavior have not been found, although it is believed that this behavior may be related to the fact that only the traditional single-parameter quadruplet mimics the positive-negative-positive signature of the interactions in each individual discrete contribution to the

interactions (i.e., for each $\boldsymbol{k}_d$).

In contrast, MDIAs based on multi-parameter quadruplet definitions but with an increased number of representative quadruplets ($N > 1$) do show stable model integration behavior for optimum parameter setting based on the optimization for selected spectra. Consequently, it appears that the more complex quadruplet definitions can only be used in practical models when multiple representative quadruplets are used.

2.d Holistic optimization

The third subject of further investigation at NCEP has been the way in which each MDIA is optimized. Traditionally, the optimization has been performed for a small number of predefined spectra. However, it has long been known that individual interactions S_{nl} are highly sensitive to small details in the spectral shape. This may well explain why Tolman (2003) found that an optimized MDIA with a two parameter (λ, μ) quadruplet definition and with 4 representative quadruplets resulted in a much better representation of S_{nl} for test spectra, yet did not appear to improve model integration notably.

Considering this, it appears to be crucial that parameterizations of S_{nl} are optimized for a broad range of spectra that actually occur in wave models. Furthermore considering that the stability of the MDIA in model integration is essential, a 'holistic' optimization approach has been developed. In this approach the parameters in the MDIA are not optimized to minimize the error of S_{nl} for selected spectra F, but to minimize errors of the spectrum F or related quantities for a set of test cases.

The WAVEWATCH III model has been set up for two standard test cases representing time and fetch limited growth for a wind speed $U_{10} = 20$ ms^{-1}. For both cases a discrete spectral grid is used with 36 directions ($\Delta\theta = 10°$) and with a frequency increment factor of 1.07 and ranging from 0.0418 to 0.417 Hz for the time limited test (35 frequencies) and from 0.040 to 0.785 Hz for the fetch limited test (45 frequencies). This spectral resolution has been adopted to assure sufficient resolution for the reference computations using the exact WRT algorithm. In the time limited test the initial conditions consist of a spectrum with a peak frequency of 0.25 Hz. The first 48 hourly spectra are used to compute model errors. In the fetch limited growth a spatial resolution of 25 km is used. Model errors are computed for 50 spectra with a fetch of up to 1250 km after 24 h of model integration.

The basic spectral output of the WAVEWATCH III model is the traditional spectrum $F(f,\theta)$, defined in terms of the frequency f and the direction θ. More robust integrated parameters obtained from this spectrum are the one dimensional frequency spectrum $F(f)$ and the significant wave height H_s

$$F(f) = \int F(f,\theta)\, d\theta \quad , \tag{10}$$

$$H_s = 4\sqrt{\int F(f)\, df} = 4\sqrt{F_t} \quad , \tag{11}$$

where F_t is the total wave energy. These three parameters are all used as the basis for error measures for the model integration. However, they all focus on the energy at the spectral peak. Particularly the high frequency flank of the spectrum, however, is important for many processes governing air-sea interactions. Additional parameters that focus more on the high frequency part of the spectrum would be the one and two dimensional steepness spectra, which are defined as $k^2F(f)$ and $k^2F(f,\theta)$, respectively. Furthermore considering that error measures should be locally normalized to give equal weight to errors at difference stages of wave growth, the following five error measures ϵ have been defined

$$\epsilon_H = \sqrt{\frac{1}{n}\sum_1^n \frac{(H_{s,x} - H_{s,a})^2}{H_{s,x}^2}}, \tag{12}$$

$$\epsilon_{e1} = \sqrt{\frac{1}{n}\sum_1^n \frac{\int \{F_x(f) - F_a(f)\}^2\, df}{F_{t,x}^2}}, \tag{13}$$

$$\epsilon_{e2} = \sqrt{\frac{1}{n}\sum_1^n \frac{\iint \{F_x(f,\theta) - F_a(f,\theta)\}^2\, df d\theta}{F_{t,x}^2}}, \tag{14}$$

$$\epsilon_{s1} = \sqrt{\frac{1}{n}\sum_1^n \frac{\int k^4 \{F_x(f) - F_a(f)\}^2\, df}{S_{t,x}^2}}, \tag{15}$$

$$\epsilon_{s2} = \sqrt{\frac{1}{n}\sum_1^n \frac{\iint k^4 \{F_x(f,\theta) - F_a(f,\theta)\}^2 df d\theta}{S_{t,x}^2}}, \tag{16}$$

where n is the number of output points considered in the optimization, where the suffices x and a denote the exact and approximated solutions, respectively, and where

$$S_t = \int k^2 F(f)\, df \quad . \tag{17}$$

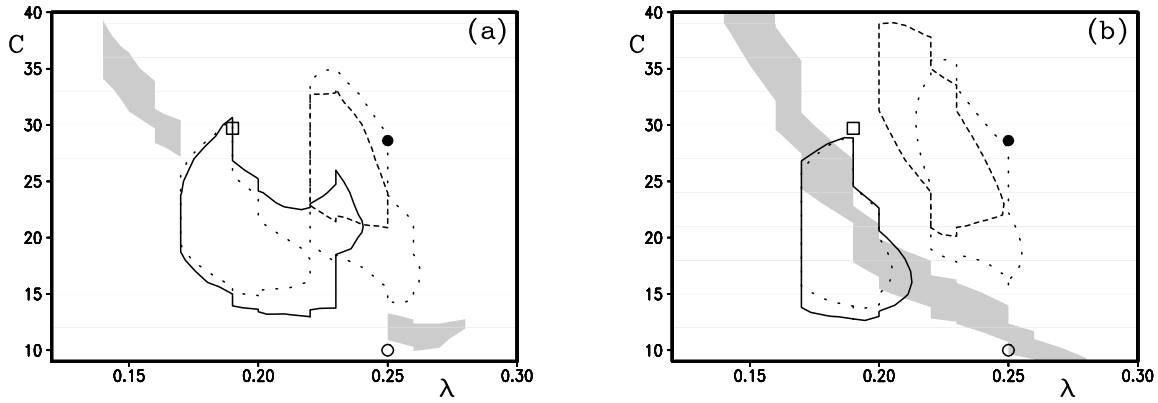

Fig. 1: Composite of error measures for the original DIA defined by λ and C. Areas in parameters space are shown where the model error is less that 1.1 times the minimum model error or 2% in total for the given parameter. Shaded area: wave heights. Solid line: one dimensional spectra $F(f)$. Dashed line: one dimensional steepness spectra $k^2F(f)$. Dotted lines: corresponding two dimensional spectra. (a) Time limited test. (b) Fetch limited test. 2% error threshold used for wave heights in panel (b) only. ∘: Tolman and Chalikov (1996) •: Hasselmann et al. (1985) □: Hashimoto and Kawaguchi (2001)

For the original DIA with the quadruplet defined by λ alone, only two parameters need to be optimized (λ and C). For this case, it is feasible to map the behavior of the different error measured in full parameter space. This is achieved by computing all error measures for λ ranging from 0.12 to 0.30 at intervals of 0.005, and C ranging from 0.9 10^7 to 4.0 10^7 at intervals of 0.1 10^7. With these results, maps of all errors ϵ have been produced (Figures not presented here). Optimum wave height errors ϵ_H were indeed found to be small (5% or less). Optimum spectral errors (ϵ_{e1} and ϵ_{e2}), however, were found to be large (of the order of 100%), whereas optimum steepness errors (ϵ_{s1} and ϵ_{s2}) were smaller, but also sizable (typically 35%).

A summary of the results is presented in Fig. 1, which identifies areas in (λ, C)-space with near-optimal behavior for the five error measures ϵ individually. The one and two dimensional spectral errors, as well as the one and two dimensional steepness spectrum errors share similar optimum areas in the parameter space. Wave height errors (shaded areas) show a fairly narrow but elongated optimum area. Note that in the time limited tests (Fig. 1a), the two optimum areas for wave heights are connected if a somewhat larger fractional increase over the lowest observed error is allowed. Optimum areas for the wave height and the spectra (ϵ_H, ϵ_{e1} and ϵ_{e2}) overlap, indicating that the wave height H_s, and the spectra $F(f)$ and $F(f,\theta)$ can be optimized simultaneously. The optimum steepness errors, however, occupy a distinctly different part of the parameters space. Hence, the traditional DIA cannot simultaneously optimize all five error measures defined here.

Also shown in Fig. 1 are three suggested combinations of (λ, C) from literature. Hasselmann et al. (1985, •) selected λ and C to accurately describe the low frequency positive lobe of $S_{nl}(f)$ for a test spectrum, accepting that this gives large errors in $S_{nl}(f)$ at higher frequencies. With the WAVEWATCH III physics used in the present tests, this results in near optimal steepness errors, but relatively poor wave height and spectral errors. Tolman and Chalikov (1996, ∘) reduced C from Hasselmann et al. (1985) to distribute errors of $S_{nl}(f)$ for their test spectra more evenly over frequency space, thus reducing the average error in $S_{nl}(f)$. In the present holistic test, this leads to near optimal results for wave heights, but in poorer behavior for spectral and steepness errors. Finally, Hashimoto and Kawaguchi (2001, □) determine an optimal (λ, C) for a somewhat larger set of test spectra. Their choice results in near-optimal wave height and spectral errors, but in more sizable steepness errors.

A similar mapping of the errors in parameter space is feasible for an MDIA with one representative quadruplet, but with more complex quadruplet definitions [(λ, μ), $(\lambda, \Delta\theta)$ or $(\lambda, \mu, \Delta\theta)$]. All of these, however, show instable integration behavior in large parts of parameter space, and will therefore not be discussed further here.

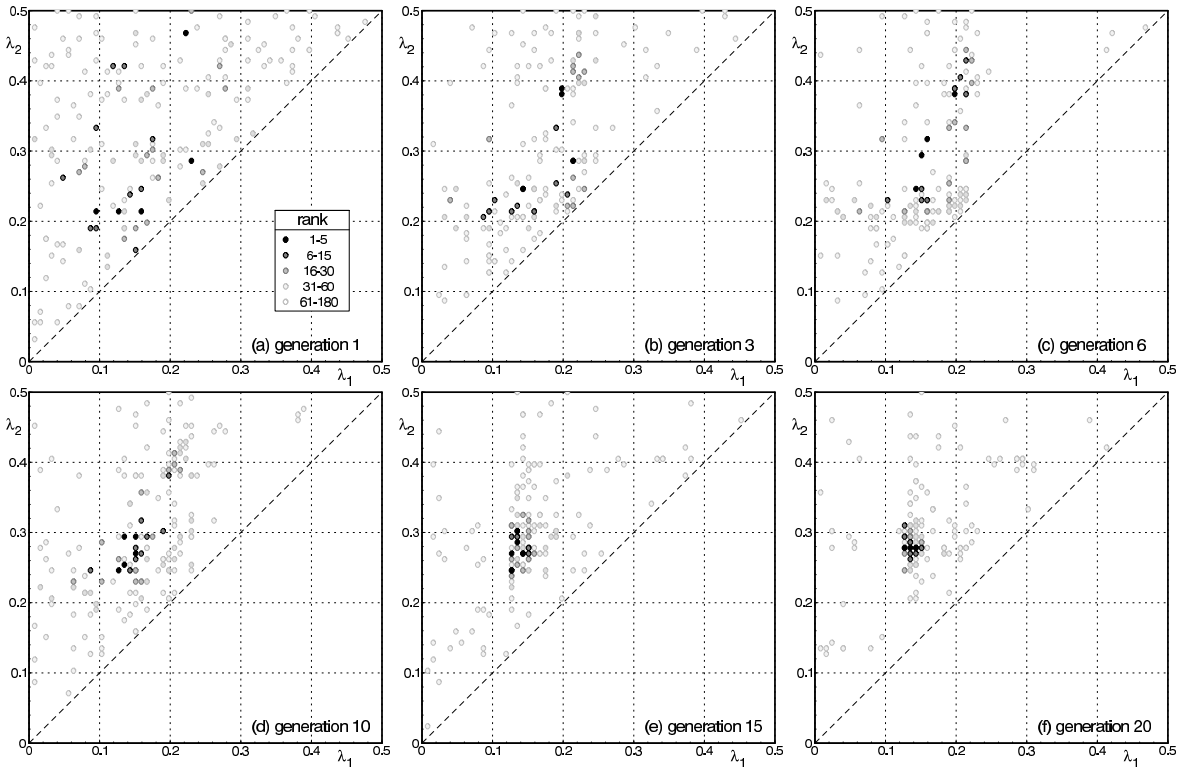

Fig. 2: Selected populations in (λ_1, λ_2) space from a genetic algorithm for an MDIA with $N = 2$ and a quadruplet defined by λ only. The rank number corresponds to the (ascending) cost function ζ.

If MDIAs with more components are considered ($N > 1$), full mapping of errors in parameter space rapidly becomes infeasible. The only alternative is then to employ a search algorithm. In such algorithms as employed in the present study, the five previously defined error measures are combined into a single cost function ζ

$$\zeta = \frac{a_H\epsilon_H + a_{e1}\epsilon_{e1} + a_{e2}\epsilon_{e2} + a_{s1}\epsilon_{s1} + a_{s2}\epsilon_{s2}}{a_H + a_{e1} + a_{e2} + a_{s1} + a_{s2}}, \quad (18)$$

where the factors a represent the weight factors. To emphasize the high accuracy that could be obtained for the wave height in the results presented above, a_H is set to 10, while all other weights are set to 1.

In a first attempt to optimize ζ for MDIAs, a traditional steepest descent method was adopted. It rapidly became clear, however, that ζ has multiple local minima for larger N, and that a descent method therefore is not appropriate to find the global minimum of ζ. Therefore, a genetic search algorithm was developed (e.g., Eiben and Smith, 2003). In such an algorithm, all parameters of the MDIA considered are described as a single string of bits. A population of such strings is then generated, from which new generations are generated using rules that are loosely based on biological evolution. Details of the genetic algorithm will be published elsewhere.

An example of results of the genetic algorithm is presented in Fig, 2. Initially, the population is randomly distributed over the valid area of (λ_1, λ_2) space (Fig. 2a). Early generations (e.g, Fig. 2c) identify local minima, where either λ_1 or λ_2 is close to the optimum value for $N = 1$ ($\lambda \approx 0.2$). Eventually (e.g, Fig. 2f) most of the population exists near the optimum values of this MDIA. Thus, by evaluating the evolution of the generations, both local and global optimum areas can be found in parameter space. Final convergence of a genetic algorithm to the global optimal solution is generally slow. Therefore, members with the lowest cost ζ of a reasonably converged population have been used as the initial conditions for a steepest descent method to estimate the actual global optimum parameters settings.

With the above optimization techniques, increasingly complex MDIAs are optimized. The resulting cost functions of the configurations investigated so far are gathered in Table. 1. Only a part of the intended experiments have been performed so far.

Table 1: Optimum cost function ζ (%) for several MDIA's as a function of the number of components N and the quadruplet definition. —: not intended for further consideration. ...: experiments planned, but not yet completed.

	quadruplet definition		
N	(λ)	(λ, μ)	$(\lambda, \mu, \Delta\theta)$
1	26.0	—	—
2	16.3	—	—
3	16.1	11.6	...
4	—	...	...
5	—	...	...

The experiments have started with the most simple possible configuration; $N = 1$ and a quadruplet defined by λ only. This is the holistically optimized original DIA, which serves as a benchmark to assess the improvements of all more complex MDIAs. The resulting cost function is dominated by the spectral errors ϵ_{e1} and ϵ_{e2}, which represent approximately 70% of the total cost function ζ. Adding a second component to this MDIA ($N = 2$) dramatically reduces the cost function from 26.0% for $N = 1$ to 16.3% for $N = 2$. Adding a third component ($N = 3$) has limited impact. Note that the corresponding experiment for $N = 4$ has been partially conducted. However, the genetic search algorithm showed that the corresponding optimum MDIA actually represented a degenerated solution with effectively $N = 3$, indicating that no further accuracy can be gained by adding more components to an MDIA with the original quadruplet definition.

Experiments with optimizing MDIAs based on the two-parameter (λ, μ) quadruplet have been started. Considering the stability issues with this quadruplet, experiments have started with an MDIA with $N = 3$. The resulting cost function again is a significant improvement over the corresponding MDIA with the traditional quadruplet definition. Moreover, the genetic search algorithm indicates that this MDIA is expected to be generally stable in a large part of parameter space around the optimum solution. It should be noted that in particular the spectral errors are greatly improved in such an MDIA. Several additional experiments are planned, and the results presented in Table 1 suggest that additional improvements might be expected for more complex MDIAs.

Table 2: MDIAs used in the intercomparison of approaches.

case	ζ (%)	λ (-)	μ (-)	$\Delta\theta$ (°)	C $\times 10^{-7}$
A	35.1	0.250	—	—	1.00
B	26.0	0.212	—	—	1.88
C	16.3	0.127	—	—	3.84
		0.278	—	—	1.83
D	11.6	0.063	0.009	—	12.1
		0.184	0.028	—	2.40
		0.284	0.128	—	5.33

To illustrate the impact of using increasingly more complex MDIAs, results of several MDIAs for the time and fetch limited test are compared to the benchmark results obtained with the WRT method. The cases considered are gathered in Table 2. Case A represents the default settings for WAVEWATCH III. Cases B through D correspond to several best fits corresponding to Table 1.

Figure 3 presents the wave height H_s as a function of time t or fetch x for the corresponding test. As already mentioned above, wave heights are described accurately using all MDIA approaches. It should nevertheless be noted that the exact solution for the time limited growth (solid line in Fig. 3a) exhibits a more distinct slowing down of the growth rate with time than any of the MDIAs. The most complex MDIA tested here (long dashed line) describes this slowing down of the growth rate systematically better than less complex approaches.

Figure 4 presents the one dimensional spectra $F(f)$ and steepness spectra $S(f) = k^2 F(f)$ after 24 h of model integration from the time limited growth test. These spectra were found to be representative for all time and fetch limited test spectra. The traditional DIA with the default settings as used in WAVEWATCH III (A, dotted lines) results in a shift of the peak frequency to higher frequencies, when compared to the reference WRT solution (solid lines). This may well explain why it has been observed frequently that WAVEWATCH III appears to underestimate peak periods for wind seas, even if the total energy (or H_s) is represented accurately. The optimized traditional DIA (B, dashed line), places the spectral peak at the proper frequency, but underestimates the peak energy density by approximately 40%, Increasing the complexity of the MDIA reduces this underestimation to just over 10% for model D.

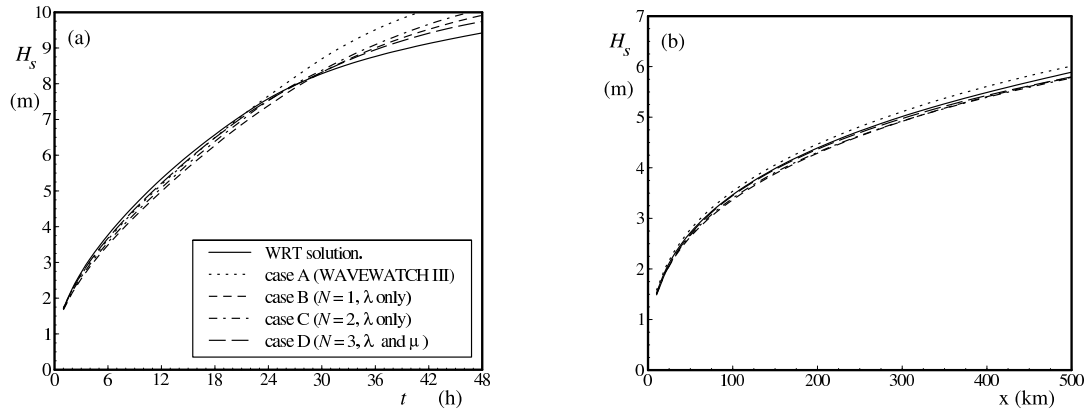

Fig. 3: Wave heights H_s as a function of (a) time t and (b) fetch x for the corresponding tests for the reference (WRT) solution and the MDIAs defined in Table 2.

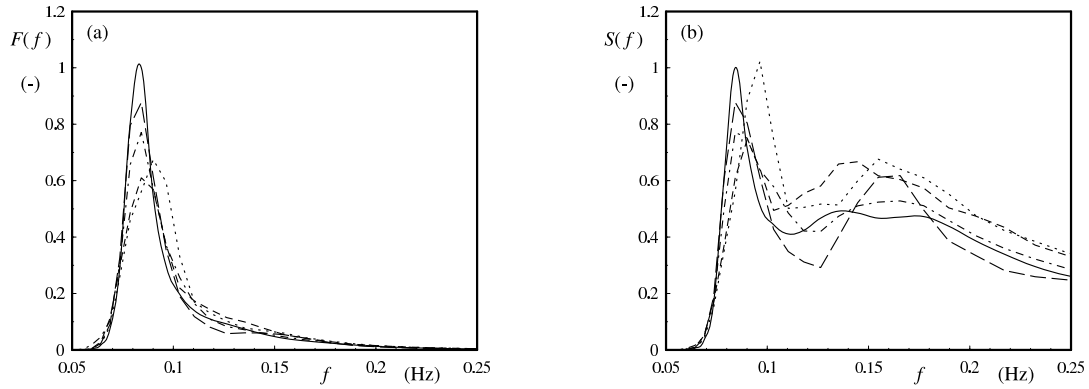

Fig. 4: One dimensional spectrum $F(f)$ (panel a) and steepness spectrum $S(f) = k^2 F(f)$ for the time limited test after 24 h. Legend as in Fig. 3. Spectra normalized with maximum value for WRT results. Legend as in Fig. 3.

An interesting additional observation can be made from the steepness spectra in Fig. 4b. Tuning, or increasing the complexity of the DIA with the traditional definition of the quadruplet (λ only, models A through C) systematically improves the quality of the modeled steepness spectra. However, going to the MDIA with the two-parameter quadruplet definition (λ and μ) and three components (model D, long dashed line), actually results in larger errors in $S(f)$ than are obtained with the less complex model C. The much more accurate description of the spectral peak in model D is accompanied by a spurious second peak in the steepness spectrum at $f \approx 0.16$ Hz.

Figure 5 presents the two dimensional spectra or spectral differences corresponding to Fig. 4a. The observed differences between MDIA versions largely correspond to differences observed in Fig. 4a, with a decreasing difference between the WRT and MDIA solutions for increasingly complex MDIAs.

2.e Outlook

The previous section presents intermediate results of a study into the optimization of MDIAs using a holistic optimization approach. Whereas the results obtained so far are promising, much work remains to be done. Several key issues still need to be addressed.

1) Finish experiments as outlined in Table 1, adding or removing experiments as deemed necessary.
2) Perform a detailed analysis of the model results, in addition to a bulk assessment through errors ϵ and the cost function ζ. If necessary, adjust weights in ζ.
3) Testing of the resulting MDIAs in more realistic conditions, in particular in turning wind cases.

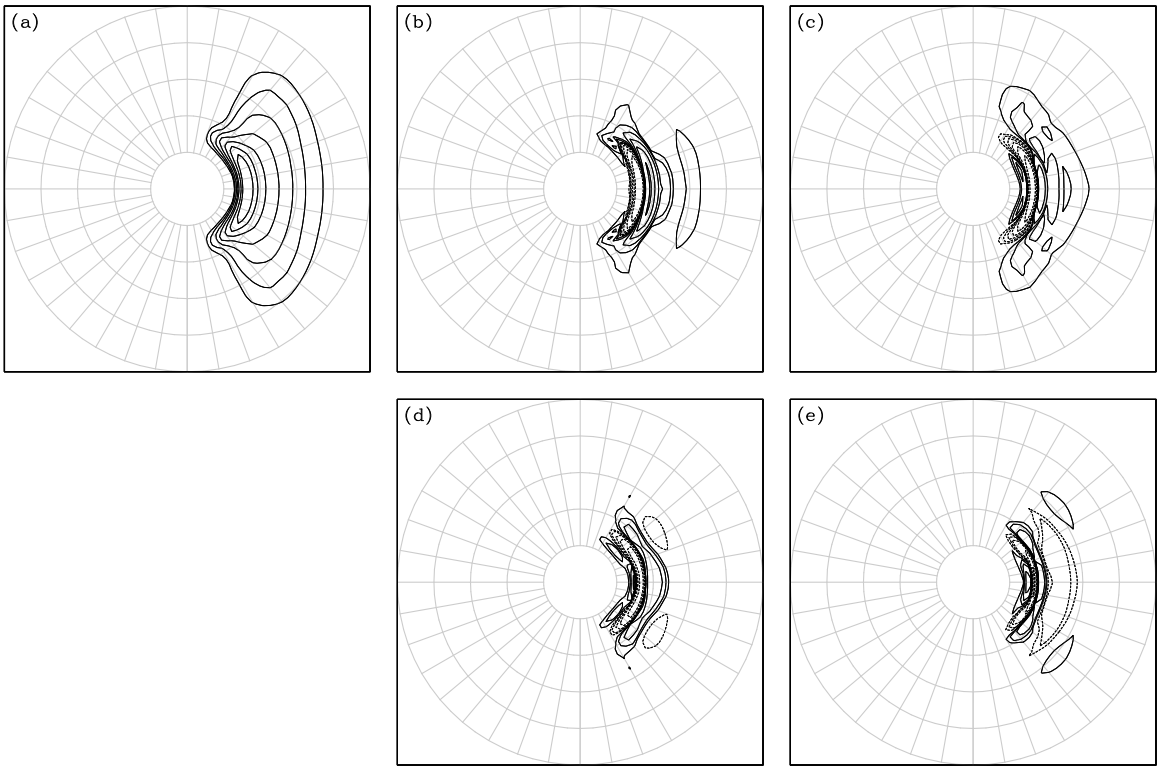

Fig. 5: (a) Reference spectrum (WRT) after 24 h from time limited test, and differences with results for models A through D (panels b through e) in Table 2. Contours at factor 2 interval with highest contour at 0.5 times the maximum spectral energy density for WRT solution. Dashed lines identify negative values. Gray lines identify spectral (f, θ) space at 0.05 Hz and 10° intervals. Differences defined as WRT - MDIA results.

This would conclude the studies as already initiated. After its conclusion, the two main issues appear to be the generalization to arbitrary depths, and the numerical optimization.

3 NEURAL NETWORKS

3.a Introduction

The development of a Neural Network Interaction Approximation (NNIA) has been pioneered by Krasnopolsky et al. (2002) and Tolman et al. (2005). In this section, a summary of their work is presented. Background references regarding Neural Networks (NNs) can be found in the above papers. Both studies focus on the feasibility of an NNIA. Considering that the most critical aspect of any interaction approximation is to reproduce wave growth in a wave model, they consider single peak spectra ('wind seas') in deep water only.

The basic precept behind the development of an NNIA is that the computation of S_{nl} from F can be viewed as a mapping problem, and that NNs are ideally suited to produce accurate and economical approximations for such problems. Krasnopolsky et al. (2002) investigated the potential of an NNIA in a feasibility study. A more mature NNIA is developed in Tolman et al. (2005). This NNIA has three basic elements; normalization, decomposition and an NN.

Before an actual NN is applied, the spectrum $F(f, \theta)$ source term $S_{nl}(f, \theta)$ frequency f and direction θ are normalized with a normalizing energy density (F_n), frequency (f_n) and direction (θ_n), resulting in the following normalized parameters

$$\tilde{F}(\tilde{f}, \tilde{\theta}) = F_n^{-1} \, F(f, \theta) \quad , \tag{19}$$

$$\tilde{S}_{nl}(\tilde{f}, \tilde{\theta}) = g^4 \, F_n^{-3} \, f_n^{-11} \, S_{nl}(f, \theta) \quad . \tag{20}$$

$$\tilde{f} = f_n^{-1} \, f \quad , \tag{21}$$

$$\tilde{\theta} = \theta - \theta_n \quad . \tag{22}$$

This normalization is performed to enforce proper scaling behavior. This scaling behavior can be included in the NN, but by using the normalized parameters the NN needs to reproduce only the proper

shape of the nonlinear interactions. This results in either a cheaper or more accurate NN. Because the present studies only consider single-peaked wind sea spectra, the obvious choices for the normalization parameters are the peak frequency, direction and energy density f_p, θ_p and F_p.

If the NN would be applied directly to $\tilde{F}$ and $\tilde{S}_{nl}$, each of the approximately 10^3 discrete spectral component needs to be mapped individually. Such a large NN is not expected to be economical. To make the NN more economical, and possibly make the NNIA less sensitive to the actual spectral resolution, the spectrum and source term are decomposed on orthogonal basis functions,

$$\tilde{F} \rightarrow \boldsymbol{X} \quad , \quad \tilde{S}_{nl} \rightarrow \boldsymbol{Y} \quad , \tag{23}$$

where $\boldsymbol{X}$ and $\boldsymbol{Y}$ represent vectors of coefficients of the basis functions (typically of the order of 10^2 or less). The actual NN is now developed to estimate $\boldsymbol{Y}$ from $\boldsymbol{X}$. In Tolman et al. (2005) Empirical Orthogonal Functions (EOFs, Lorenz, 1956; Jolliffe, 1986) were established as efficient basis functions for the NNIA. Note that with the adoption of EOFs, this NNIA can be considered as a generalization of the EOF based approach discussed in Hasselmann et al. (1985).

The development of an NN (or NNIA) consists of a process called training. In this process, the NN is optimized using a large set of spectra and the corresponding exact (WRT) interactions. In the early studies, parametric wind sea spectra have been used to assure that the training is based on a broad envelope of possible wind sea spectra. From this training data set, EOFs are determined first. Second, the NN is trained using the corresponding vectors $\boldsymbol{X}$ and $\boldsymbol{Y}$. Note that the training process can be extremely expensive, but that the resulting NN (NNIA) is generally economical.

Tolman et al. (2005) show that such an NNIA can accurately describe interactions for spectra similar to those used for the training. Moreover, reasonable results are obtained for wind sea spectra obtained from WAVEWATCH III. The cost of such an NNIA proved comparable to that of the DIA, with nearly all the computational effort spend in the decomposition of $\tilde{F}$ into $\boldsymbol{X}$ and the recomposition of $\tilde{S}_{nl}$ from $\boldsymbol{Y}$.

In spite of the positive results from these studies, the resulting NNIA is not (expected to be) able to result in stable model integration when applied in a wave model like WAVEWATCH III. The reason for this failure is that spectra in a wave model include peculiarities that are not present in the parametric spectra used to train the NNIA. In such conditions, the NNIA will 'extrapolate' rather than 'interpolate', and cannot be expected to give accurate results.

3.b Recent developments

Ongoing research at NCEP focuses on developing an NNIA that will result in stable and accurate wave growth computation when applied in WAVEWATCH III. Considering the previous section, the logical first step to achieve this goal is to develop a training data set that consists of modeled wave spectra. Such a training data set is generated by the WAVEWATCH III model with the WRT exact interaction approach considering a variety of time limited wave growth computations according to Eq. (9). Several runs are made with either constant, or slowly and randomly varying winds. To obtain a rich data set, each individual spectrum and source term of these calculations is included in the training data set.

Even if this more appropriate training data set is used, it is doubtful that such a training data set can ever encompass all possible wind sea spectra that can occur in the wave model. It is therefore doubtful that the corresponding NNIA will be able to produce the level of robustness necessary for incorporation in a practical wave model. However, a hybrid NNIA can be developed if it is possible to estimate objectively when the NNIA becomes inaccurate ('fails'). In such a case the hybrid NNIA could revert to an alternative estimate for S_{nl}, until the actual NN approach becomes sufficiently accurate again.

A method to objectively estimate the quality of a NN estimate has been pioneered by Krasnopolsky and Schiller (2003). Next to the NN that estimates $\boldsymbol{Y}$ from $\boldsymbol{X}$, and inverse NN (iNN) is developed that estimates $\boldsymbol{X}$ from $\boldsymbol{Y}$. If the latter estimate is denoted as $\boldsymbol{X}'$, the similarity between $\boldsymbol{X}$ and $\boldsymbol{X}'$ becomes a measure for the accuracy of the NN (NNIA). In our case, an appropriate error measure ϵ is the normalized rms difference between the basis function coefficients $\boldsymbol{X}$ and $\boldsymbol{X}'$. The corresponding hybrid NNIA (HNNIA) based on the WRT method is illustrated in Fig. 6. The process of testing the accuracy of the NNIA is denoted as the quality control or QC.

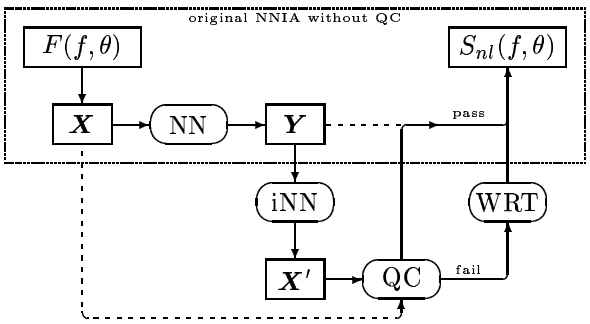

Fig. 6: Layout of the hybrid NNIA (HNNIA), reverting to the WRT algorithm in cases where the quality control (QC) indicates failure of the NN. Note that $\boldsymbol{X}$ and $\boldsymbol{Y}$ contain decomposition coefficients for the normalized spectrum $\tilde{F}$ and source $\tilde{S}_{nl}$.

The introduction of the HNNIA serves two purposes. First and foremost, it is intended to provide robustness to the algorithm when applied in a general wave model. Second, it can be used to iteratively expand the training data set for the NNIA in the following way. Initially, the NNIA is trained with the original training data set. After the corresponding HNNIA has been developed, it is applied to the same test cases that were used to generate the training data set. All spectra for which the QC indicates failure are saved together with their exact interaction, and these data are added to the training data set. With this expanded training data set a new version of the (H)NNIA is developed, and the above process can be repeated.

Good progress has been made at NCEP with the development of an actual HNNIA. A first training data set was constructed using 15 time limited growth cases as described above, resulting in a training data set of approximately 5000 spectra F and source terms S_{nl}. The HNNIA developed with this first training data set has been implemented in WAVEWATCH III. Figure 7 shows spectra at the end of a growth test with a constant wind speed of 26.8 ms^{-1} as obtained with this HNNIA for various maximum allowed errors $\epsilon_{\max}$ in the QC. Note that this represents the first test case used to generate the training data set.

Figure 7a shows results for a NNIA without QC. Obviously, this algorithm does not result in acceptable model spectra. With increasingly aggressive QC (Figs. 7b through e), the resulting spectra and wave heights converge to the exact solution as presented in Fig. 7f. Note that even for $\epsilon_{\max} = 2.5\%$ the NNIA is accepted for more than 50% of the spectra. Although there are still clear deficiencies in the HNNIA based spectra, particularly for larger values of $\epsilon_{\max}$, these results clearly provide proof of concept for the HNNIA. Nevertheless, these are only preliminary results, and much work remains to be done. Our future plans in this respect are presented in the following section.

3.c Outlook

The most obvious deficiency of the the HNNIA with finite values of $\epsilon_{\max}$ is the 'hole' in the spectrum at frequencies between 2 and 3 times f_p and roughly in the wind direction. We are presently investigating if this behavior can be suppressed by increasing the accuracy of the NNIA in this frequency range. The latter can be achieved by properly weighting errors as a function of the frequency f in the training of the NN in the NNIA. We furthermore intend to investigate the following aspects of this HNNIA:

1) We need to establish if the iterative expansion of the training data set indeed increases the robustness of the NNIA, and the economy and accuracy of the HNNIA.

2) Close observation of the model integration results obtained with the HNNIA suggest that the NNIA systematically reduces time steps in WAVEWATCH III whereas the WRT algorithm increases time steps. This suggests that the NNIA introduces noise in the spectrum, which is removed by the WRT algorithm when the QC activates the WRT algorithm. We intend to investigate the source and spectral representation of such noise, and will consider adding an explicit diffusion element to the NNIA to suppress such noise.

3) The resulting HNNIA will need to be tested using independent test cases (Fig. 7 was obtained for one of the training cases), and the robustness of the HNNIA needs to be demonstrated for conditions where the assumption of unimodal wind sea spectra is clearly violated.

If the above issues can be addressed satisfactorily, the potential of the HNNIA has been clearly established. The next step then will be to develop a HNNIA for arbitrary spectra (including swell) and arbitrary depths. Such an HNNIA should be trained with, and applied to realistic wave model applications.

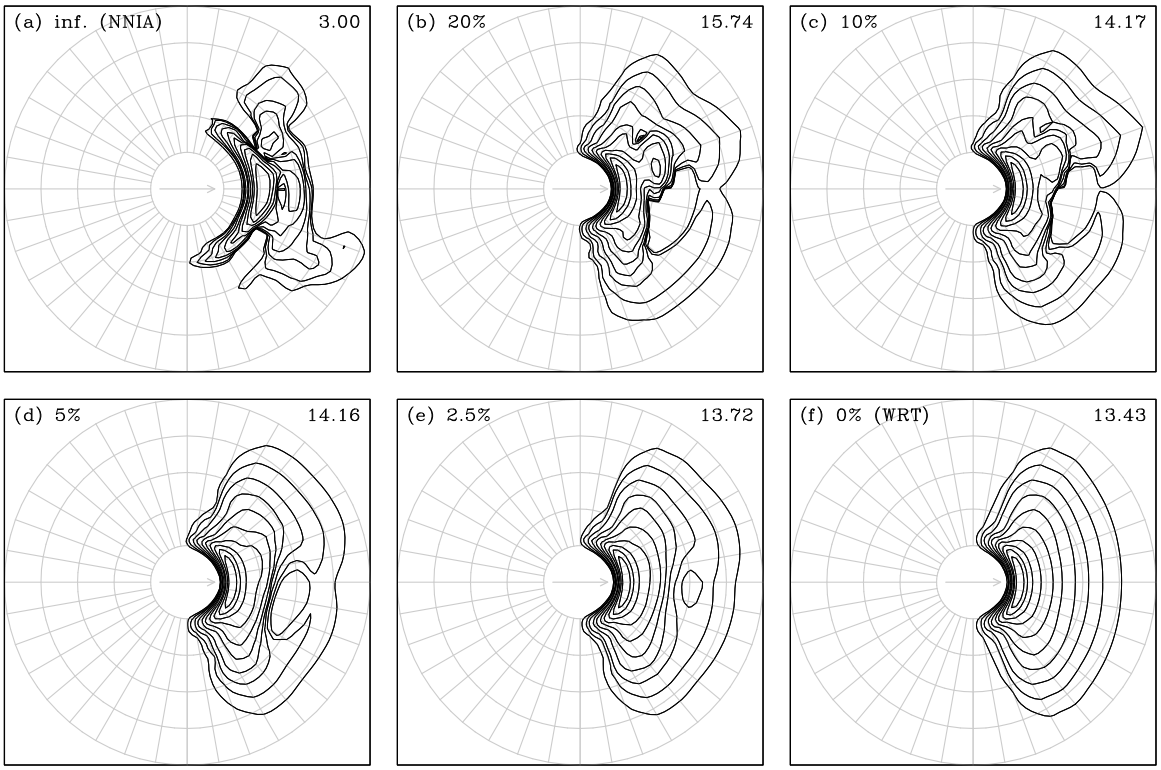

Fig. 7: Polar plot representation of spectra $F(f,\theta)$ at the end of a time limited growth test with a constant wind speed of 26.8 ms^{-1} obtained with WAVEWATCH III and the first version of the HNNIA. Contours at factor 2 intervals, starting with the local peak energy density in the spectrum. Wave height H_s in m are presented in the upper right corner of the panels. Arrows identify the wind direction. Gray lines identify spectral (f,θ) space at 0.05 Hz and 10° intervals. Results for various values of the maximum allowed error $\epsilon_{\max}$ in the QC as identified in upper left corner panels. Panels (a) and (f) represent the pure NNIA and WRT solutions, respectively.

4 OUTLOOK

The present manuscript presents an brief overview of recent studies into the modeling of nonlinear interactions in wind wave models. and a more in depth presentation of recent results obtained in this field at NCEP. Third generation wave models, in which the nonlinear interactions are explicitly accounted for, became feasible for practical wave modeling with the development of the DIA (Hasselmann et al., 1985). Although the DIA was very successful in this respect, its shortcoming were already identified in the original paper. Much effort has been spend on finding an more accurate yet economical alternative to the DIA. With the ever increasing computational power available, more expensive methods are becoming feasible.

Two possible alternatives to the DIA have been identified. The first is the SRIAM method (Hashimoto and Kawaguchi, 2001), which represents a reduced version of the exact interactions. This method appears accurate for test spectra, but, to the knowledge of the present authors, has not been tested rigorously as part of a practical wave model. The second methods is based on describing the interactions as a diffusion process (Zakharov and Pushkarev, 1999; Jenkins and Phillips, 2001). The first of these papers establishes this approach as feasible in a wave model, however, a rigorous assessment of the accuracy of such an approach does not appear to have been made. The present study provides a framework of holistic testing or optimization of these approaches, which will become essential in comparing these methods to alternatives presented here.

The first alternative to the DIA considered in detail here is the expansion of the traditional DIA. Such an approach has been advocated by many previous authors, as reviewed in Section 1. The present study presents a holistic method to optimize alternative DIAs. It is shown that by expanding the number of representative quadruplets, and by expanding the definition of the representative quadruplet, the performance of the DIA (MDIA) can be improved dramatically. Ongoing research in this direction is designed to probe how far this improvement can go.

By performing the (M)DIA optimization, it became clear that the parameter settings of the DIA as used in the WAVEWATCH III model are responsible for systematic errors in the peak frequency or period for this model for wind seas. With the results presented here, one might be tempted to simply use the optimized parameter settings of the corresponding DIA in this model. However, such an approach is not expected to improve the behavior of WAVEWATCH III, because all other source terms are designed / tuned to work with the default DIA settings of this model. Hence, introducing a more appropriate DIA in WAVEWATCH III will require a reconsideration or retuning of all other source terms.

Furthermore, this study shows the potential of Hybrid Neural Network Interaction Approximation (HNNIA) in actual wave model integration. However, much work still needs to be done in this field, as identified in Section 3.c.

Finally, the new work presented here opens another potential avenue of attempting to improve the description of the nonlinear interactions in practical wave models. In principle it appears possible to dynamically adjust the parameters of a DIA depending on the actual input spectrum. A natural way to do this would be a by using a NN. Alternatively, more of the interaction physics could be built into the NNIA, by using DIA solutions as 'basis functions'. Both approaches would result in a Neural Network Discrete Interaction Approximation (NNDIA), which we intend to pursue further.

References

Eiben, A. E. and J. E. Smith, 2003: *Introduction to Evolutionary Computing*. Springer, 299 pp.

Hashimoto, N. and K. Kawaguchi, 2001: Extension and modification of Discrete Interaction Approximation (DIA) for computing nonlinear energy transfer of gravity wave spectrum. in *Ocean Wave Measurement and Analysis*, pp. 530–539. ASCE.

Hasselmann, K., 1960: Grundgleichungen der seegangsvoraussage. *Schiffstechnik*, **1**, 191–195.

Hasselmann, K., 1962: On the non-linear transfer in a gravity wave spectrum, Part 1. General theory. *J. Fluid Mech.*, **12**, 481–500.

Hasselmann, K., 1963a: On the non-linear transfer in a gravity wave spectrum, Part 2, Conservation theory, wave-particle correspondence, irreversibility. *J. Fluid Mech.*, **15**, 273–281.

Hasselmann, K., 1963b: On the non-linear transfer in a gravity wave spectrum, Part 3. Evaluation of energy flux and sea-swell interactions for a Neuman spectrum. *J. Fluid Mech.*, **15**, 385–398.

Hasselmann, K., T. P. Barnett, E. Bouws, H. Carlson, D. E. Cartwright, K. Enke, J. A. Ewing, H. Gienapp, D. E. Hasselmann, P. Kruseman, A. Meerburg, P. Mueller, D. J. Olbers, K. Richter, W. Sell and H. Walden, 1973: Measurements of wind-wave growth and swell decay during the Joint North Sea Wave Project (JONSWAP). *Ergaenzungsheft zur Deutschen Hydrographischen Zeitschrift, Reihe A(8)*, **12**, 95 pp.

Hasselmann, S., K. Hasselmann, J. H. Allender and T. P. Barnett, 1985: Computations and parameterizations of the nonlinear energy transfer in a gravity-wave spectrum, Part II: parameterizations of the nonlinear energy transfer for application in wave models. *J. Phys. Oceanogr.*, **15**, 1378–1391.

Herterich, K. and K. Hasselmann, 1980: A similarity relation for the nonlinear energy transfer in a finite-depth gravity-wave spectrum. *J. Fluid Mech.*, **97**, 215–224.

Jenkins, A. and O. M. Phillips, 2001: A simple formula for nonlinear wave-wave interactions. *Int. J. Offshore Polar Eng.*, **11**, 81–86.

Jolliffe, I., 1986: *Principle Component Analysis*. Springer Verlag.

Komatsu, K. and A. Masuda, 1996: A new scheme of nonlinear energy transfer among wind waves: RIAM method – algorithm and performance. *Journal of Oceanography*, **52**, 509–537.

Komen, G. J., L. Cavaleri, M. Donelan, K. Hasselmann, S. Hasselmann and P. E. A. M. Janssen, 1994: *Dynamics and modelling of ocean waves*. Cambridge University Press, 532 pp.

Krasnopolsky, V. M., D. V. Chalikov and H. L. Tolman, 2002: A neural network technique to improve computational efficiency of numerical oceanic models. *Ocean Mod.*, **4**, 363–383.

Krasnopolsky, V. M. and H. Schiller, 2003: Some neural network applications in environmental sci-

ences part I: Forward and inverse problems in geophysical remote measurements. *Neural Networks*, **16**, 321–334.

Lorenz, E. N., 1956: Empirical orthogonal functions and statistical weather prediction. Sci. Rep. 1, MIT Cambridge, Statisical Forecasting Project, 48 pp.

Masuda, A., 1980: Nonlinear energy transfer between wind waves. *J. Phys. Oceanogr.*, **10**, 2082–2093.

Phillips, O. M., 1960: On the dynamics of unsteady gravity waves of finite amplitude. *J. Fluid Mech.*, **9**, 193–217.

Phillips, O. M., 1981: Wave interactions: the evolution of an idea. *J. Fluid Mech.*, **106**, 215–227.

Polnikov, V. G., 2003: The choice of optimal Discrete Interaction Approximation to the kinetic integral for ocean waves. *Nonlinear Proc. Geoph.*, **10**, 425–434.

Polnikov, V. G. and L. Farina, 2002: On the problem of optimal approximation of the four-wave kinetic integral. *Nonlinear Proc. Geoph.*, **9**, 497–512.

Resio, D. T. and W. Perrie, 1991: A numerical study of nonlinear energy fluxes due to wave-wave interactions. Part 1: Methodology and basic results. *J. Fluid Mech.*, **223**, 609–629.

Snyder, R. L., R. B. Long and W. L. Neu, 1998: A fully nonlinear regional wave model for the Bight of Abaco 1. Nonlinear-transfer computation. *J. Geophys. Res.*, **103**, 3119–3141.

Tolman, H. L., 2002: User manual and system documentation of WAVEWATCH III version 2.22. Tech. Note 222, NOAA/NWS/NCEP/MMAB, 133 pp.

Tolman, H. L., 2003: Optimum Discrete Interaction Approximations for wind waves. Part 1: Mapping using inverse modeling. Tech. Note 227, NOAA/NWS/NCEP/MMAB, 57 pp. + Appendices.

Tolman, H. L., 2004: Inverse modeling of Discrete Interaction Approximations for nonlinear interactions in wind waves. *Ocean Mod.*, **6**, 405–422.

Tolman, H. L., B. Balasubramaniyan, L. D. Burroughs, D. V. Chalikov, Y. Y. Chao, H. S. Chen and V. M. Gerald, 2002: Development and implementation of wind generated ocean surface wave models at NCEP. *Wea. Forecasting*, **17**, 311–333.

Tolman, H. L. and D. V. Chalikov, 1996: Source terms in a third-generation wind-wave model. *J. Phys. Oceanogr.*, **26**, 2497–2518.

Tolman, H. L., V. M. Krasnopolsky and D. V. Chalikov, 2005: Neural Network approximations for nonlinear interactions in wind wave spectra: direct mapping for wind seas in deep water. *Ocean Mod.*, In Press.

Tracy, B. and D. T. Resio, 1982: Theory and calculation of the nonlinear energy transfer between sea waves in deep water. WES Report 11, US Army Corps of Engineers.

Ueno, K. and M. Ishizaka, 1997: On an efficient calculation method of the nonlinear energy transfer in wind waves. *Sottukojiho, JMA*, **64**, 75–80, (In Japanese).

Van Vledder, G. Ph., 2000: Improved method for obtaining the integration space for the computation of nonlinear quadruplet wave-wave interaction. in *Proceedings of the 6th International Workshop on Wave Forecasting and Hindcasting*, pp. 418–431.

Van Vledder, G. Ph., 2001: Extension of the Discrete Interaction Approximation for computing nonlinear quadruplet wave-wave interactions in operational wave prediction models. in *Ocean Wave Measurement and Analysis*, pp. 540–549. ASCE.

Van Vledder, G. Ph., 2002a: Improved parameterizations of nonlinear four wave interactions for application in operational wave prediction models. Report 151a, Alkyon, The Netherlands.

Van Vledder, G. Ph., 2002b: A subroutine version of the Webb/Resio/Tracy method for the computation of nonlinear quadruplet interactions in a wind-wave spectrum. Report 151b, Alkyon, The Netherlands.

WAMDIG, 1988: The WAM model – a third generation ocean wave prediction model. *J. Phys. Oceanogr.*, **18**, 1775–1809.

Webb, D. J., 1978: Non-linear transfers between sea waves. *Deep-Sea Res.*, **25**, 279–298.

Young, I. R. and G. Ph. Van Vledder, 1993: A review of the central role of nonlinear interactions in wind-wave evolution. *Trans. Roy. Soc. London*, **342**, 505–524.

Zakharov, V. E. and A. N. Pushkarev, 1999: Diffusion model of interacting graviry waves on the surface of a deep fluid. *Nonlinear Proc. Geoph.*, **6**, 1–10.